Dispersion of asphaltenes in petroleum with ionic liquids-evaluation of molecular interactions in the binary mixture

Adeniyi S. Ogunlaja, Eric Hosten and Zenixole R. Tshentu*

Department of Chemistry, Nelson Mandela Metropolitan University, P.O. Box 77000, Port-Elizabeth 6031, South Africa

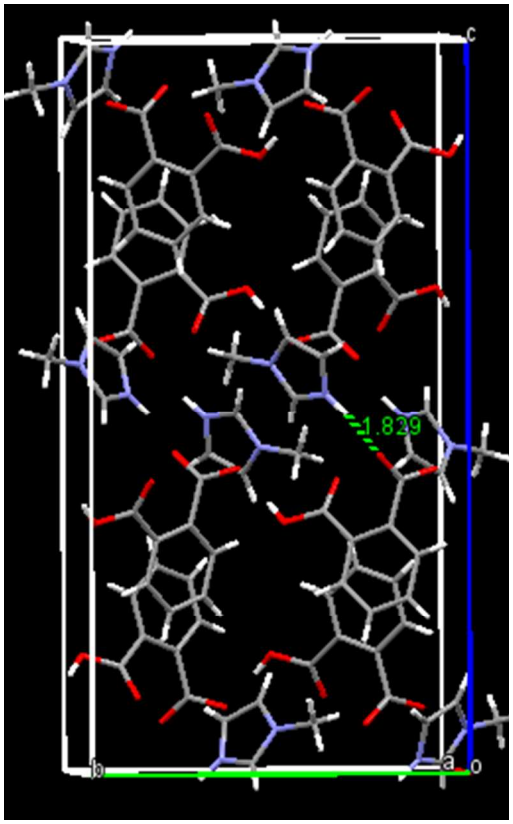

Figure S1. Crystal packing of 1-methyl-1*H*-imidazol-3-ium 2-carboxybenzoate showing short N(22)-H...O(14) contacts of 1.83 Å.

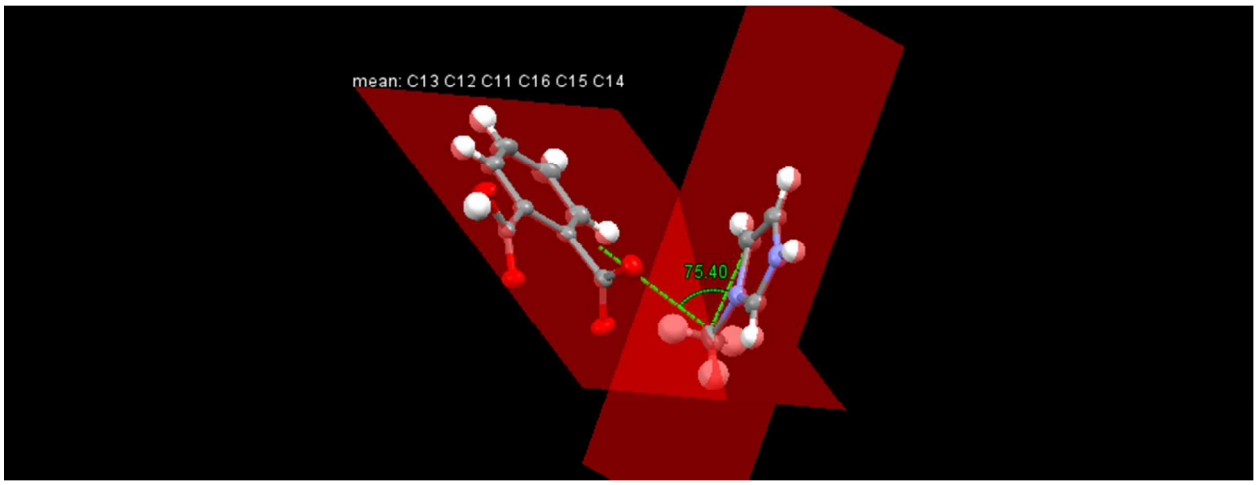

Figure S2. Structure of 1-methyl-1*H*-imidazol-3-ium 2-carboxybenzoate showing the angular plane between the imidazolium cation and carboxylate anion.

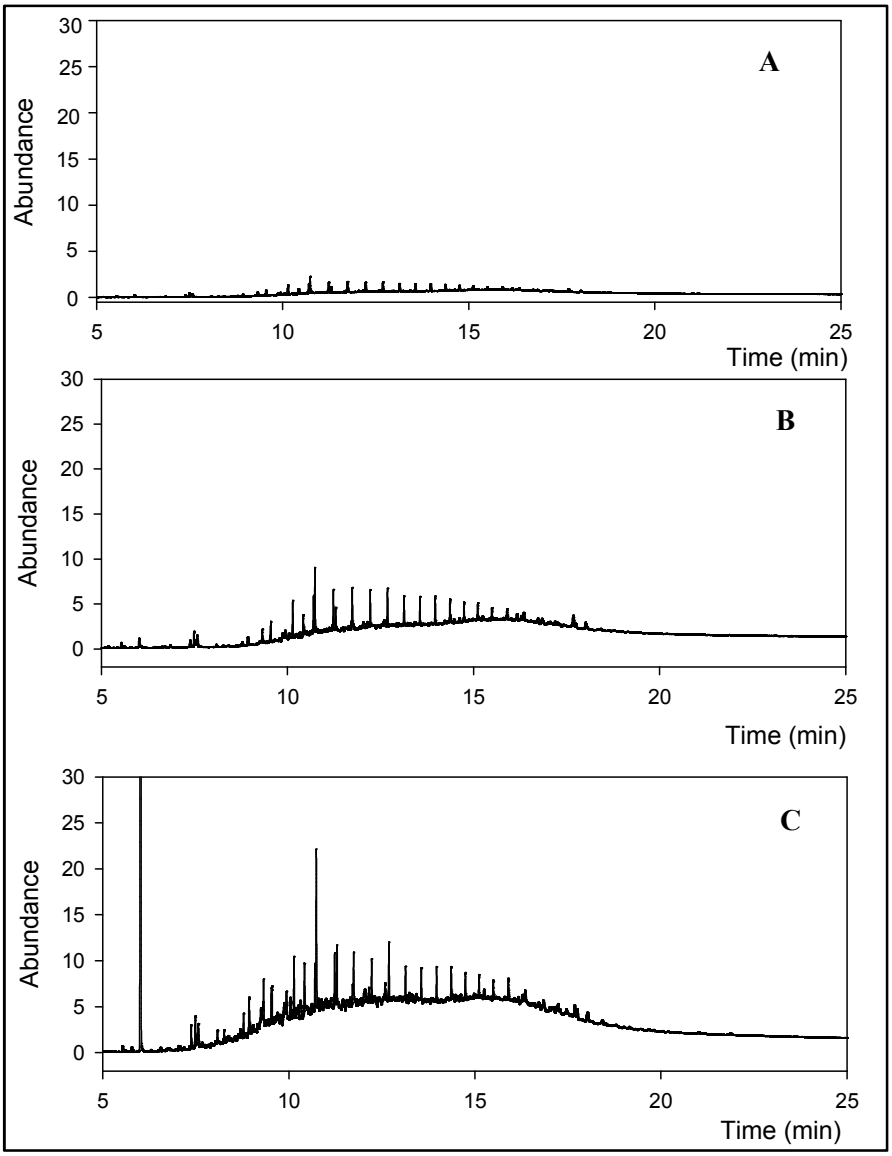

Figure S3. GC-FID chromatograms of precipitates obtained when employing 1-butyl-3-methylimidazolium chloride of (A) 9 equiv (B) 5 equiv. and (C) 2 equiv.

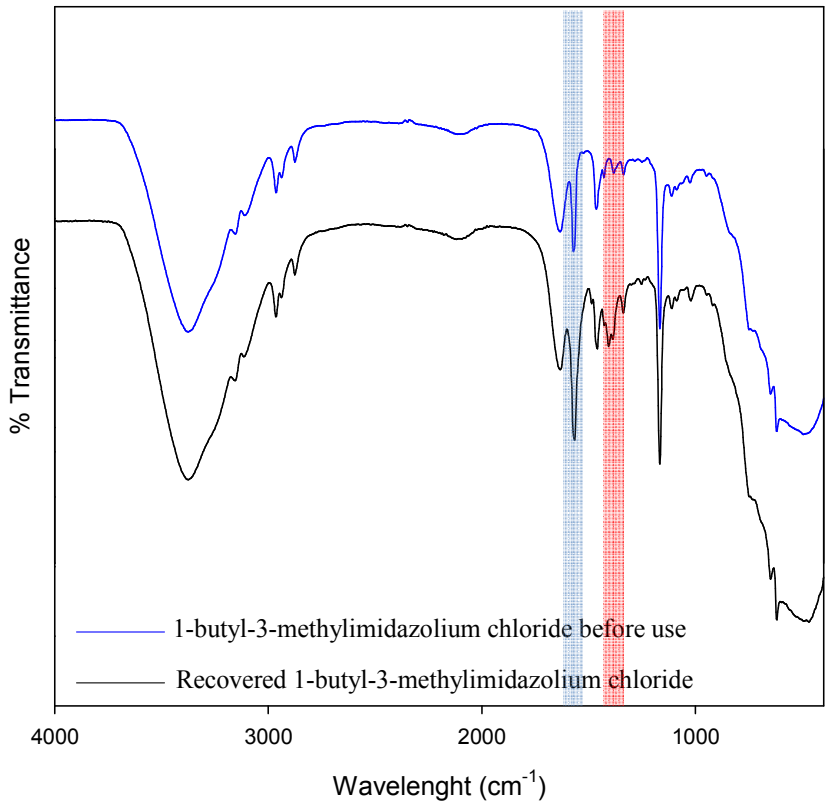

Figure S4. FT-IR of 1-butyl-3-methylimidazolium chloride before and after use (recovered). The recovered 1-butyl-3-methylimidazolium chloride gave two characteristic new bands. The blue line around 1574 cm^{-1} show an increase in the intensity of the -C=C- bands of the ionic liquid and the red line show the appearance of a new band around 1379 cm^{-1} which is characteristic of the C-N band attributed to asphaltenes.

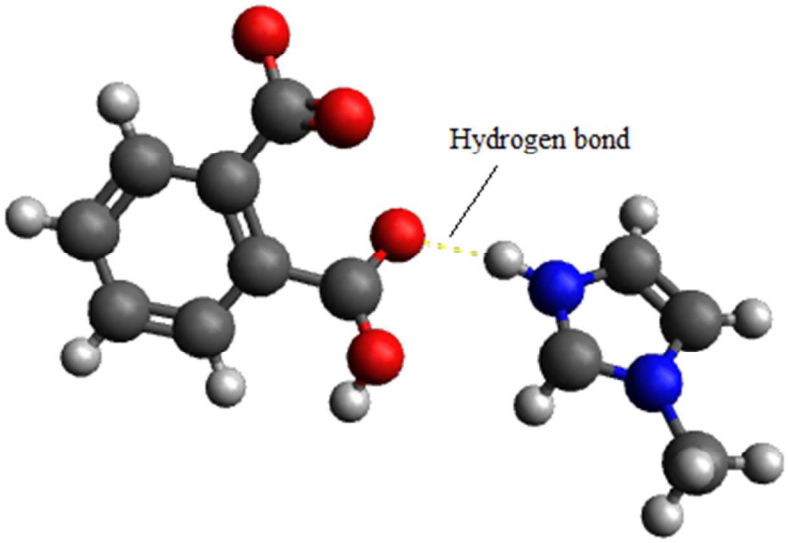

Figure S5. Optimised geometry of 1-methyl-1*H*-imidazol-3-ium 2-carboxybenzoate showing hydrogen bonding interaction (Avogadro software).

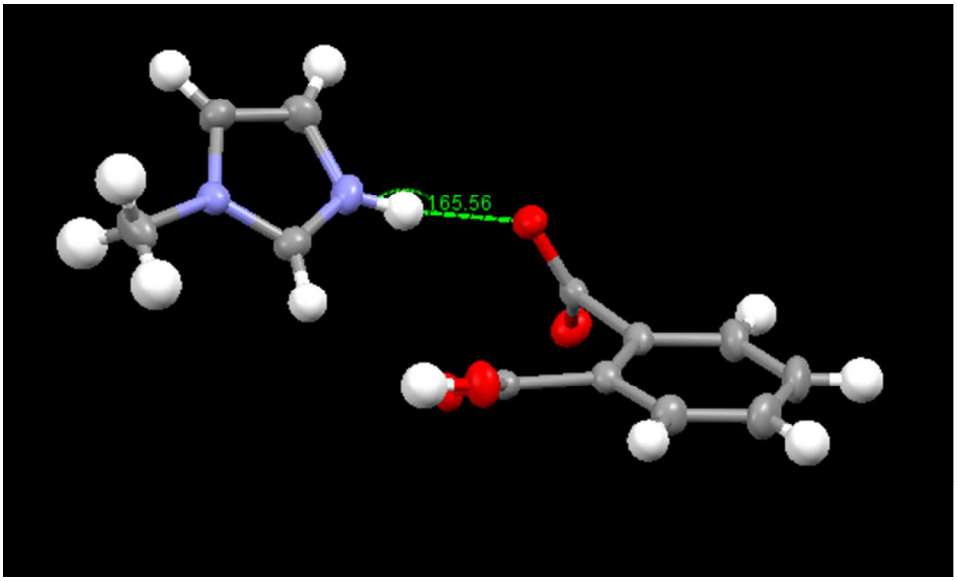

Figure S6. A contact angle between the cation and anion of 1-methyl-1H-imidazol-3-ium 2-carboxybenzoate

Table S1. DFT molecular modelling thermodynamic data (Δ*H and* Δ*G*) of ionic liquids 1-butyl-3-methylimidazolium chloride, 1-butyl-3-methylimidazolium nitrate, 1-methyl-1*H*-imidazol-3-ium-2-carboxybenzoate and asphaltenes.

	ΔH (kcal.mol^{-1})	ΔG (kcal.mol^{-1})
1-butyl-3-methylimidazolium chloride	-554291.2	-554326.5
1-butyl-3-methylimidazolium nitrate	-441389.6	-441429.2
1-methyl-1*H*-imidazol-3-ium-2-carboxybenzoate	-548864.1	-548905.8
Asphaltenes	-1939021.3	-1939112.1

Molecular modelling data for proposed asphaltene structure 2.

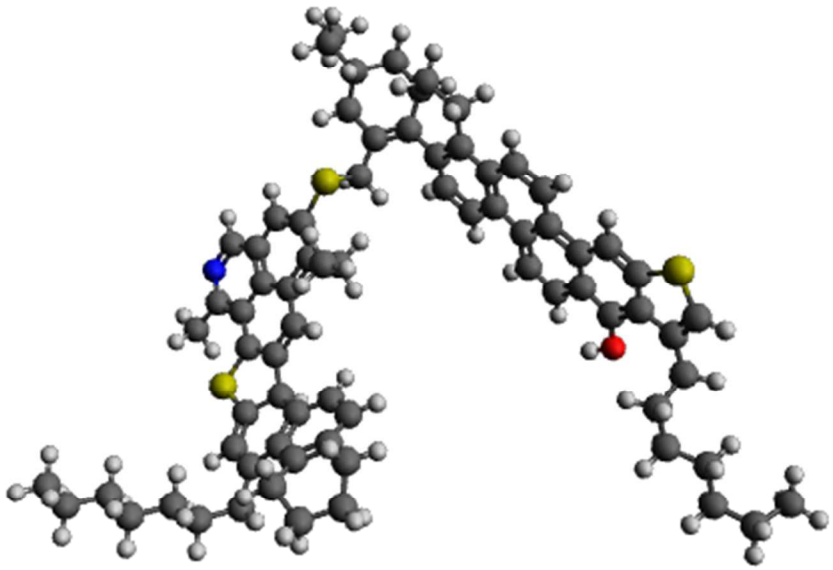

Figure S7. Structure of proposed asphaltene (2). Red, blue, yellow and grey colours represent oxygen, nitrogen, sulfur and carbon atoms respectively

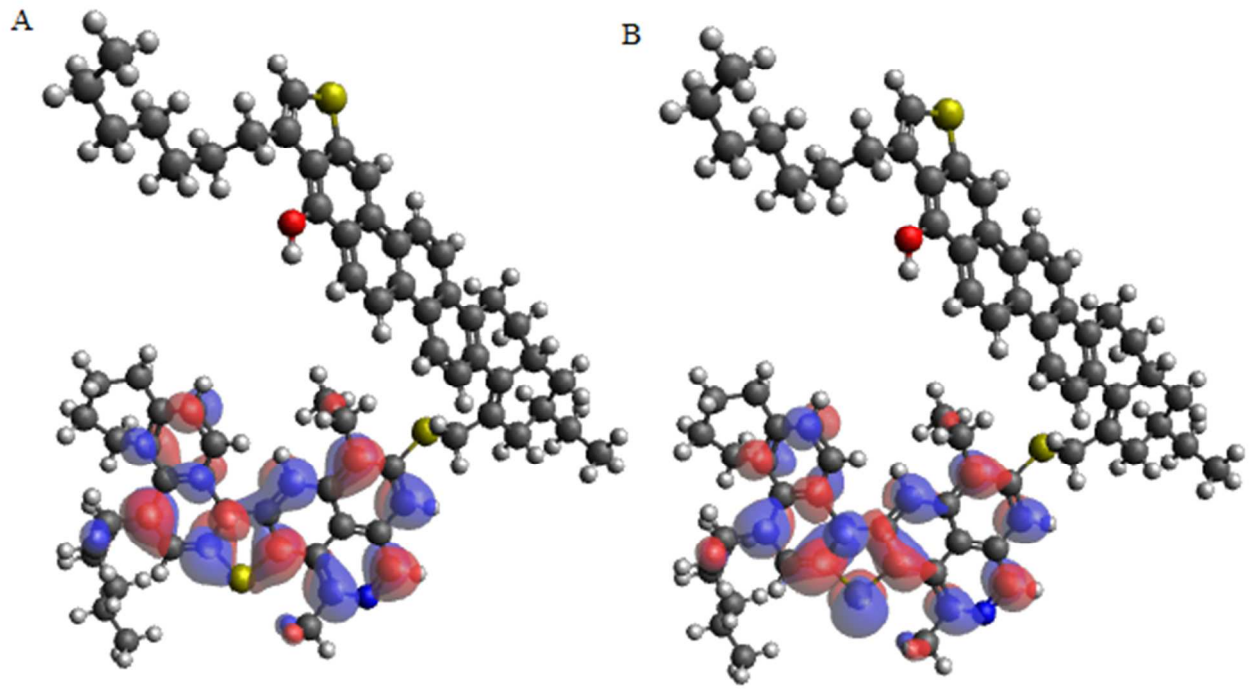

Figure S8. HOMO and LUMO locations of proposed asphaltene structure 2: (a) HOMO and (b) LUMO. Red, blue, yellow and grey colours represent oxygen, nitrogen, sulfur and carbon atoms respectively

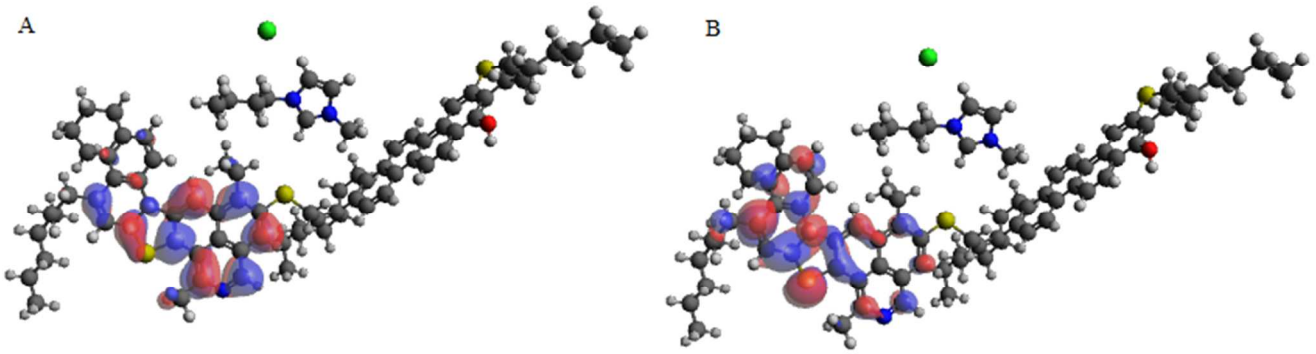

Figure S9. HOMO and LUMO locations of adduct formed between asphaltene (2) and 1-butyl-3-methylimidazolium chloride: (a) HOMO and (b) LUMO. Red, blue, yellow and grey colours represent oxygen, nitrogen, sulfur and carbon atoms respectively

Table S2. HOMO (E_H) and LUMO (E_L) energies for asphaltenes 2 and Asphaltene (2)-1-butyl-3-methylimidazolium chloride adduct.

Compounds	E_H (eV)	E_L (eV)	Orbital Energy Gap. (E_G) (eV)
Asphaltene (2)	-3.88	-2.70	1.18
Asphaltene (2)-1-butyl-3-methylimidazolium chloride adduct	-5.04	0.13	5.17

Table S3. DFT molecular modelling thermodynamic data (ΔH and ΔG) of asphaltenes (2) and adduct formed between 1-butyl-3-methylimidazolium chloride and asphaltene (2).

	ΔH (kcal.mol^{-1})	ΔG (kcal.mol^{-1})
Asphaltene (2)	-29.3×10^5	-26.3×10^5

Table S4. DFT molecular modelling thermodynamic data ($\Delta\Delta H$, $\Delta\Delta G$ and $\Delta\Delta S$) on the formation of adduct between 1-butyl-3-methylimidazolium chloride and asphaltenes (2).

	$\Delta\Delta$H (kcal.mol^{-1})	$\Delta\Delta$G (kcal.mol^{-1})	$\Delta\Delta$S (cal.mol^{-1})
Adduct (2)	16.045×10^3	16.058×10^3	-43.624

Table S5. Electrostatic charge transfer between 1-butyl-3-methylimidazolium chloride and asphaltenes (2)

1-butyl-3-methylimidazolium chloride		
Atom	Before adduct was formed	After adduct was formed
N(1)	-0.335	-0.424
N(2)	-0.330	-0.419
Cl	-0.863	-0.971
Asphaltenes (2)		
Atom	Before adduct was formed	After adduct was formed
S(1)	0.559	0.688
S(2)	0.211	0.216
S(3)	0.412	0.379
N(1)	-0.459	-0.492
O(1)	-0.693	-0.770